Research in Molecular Medicine

Research Paper

Immunoinformatics-guided Design and Structural Validation of a Multi-epitope Vaccine Candidate Targeting Gastric Cancer–associated Membrane Proteins

Kianoush Mohammadi[1], Reza Safaralizadeh[1*], Elham Safarzadeh[2], Ali Shamsazar[3]

1. Department of Animal Biology, Faculty of Natural Sciences University of Tabriz, Tabriz, Iran.
2. Cancer Immunology and Immunotherapy Research Center, Ardabil University of Medical Sciences, Ardabil, Iran.
3. Department of Biology, Faculty of Science, University of Mohaghegh Ardabili, Ardabil, Iran.

Use your device to scan and read the article online

Citation Mohammadi K, Safaralizadeh R, Safarzadeh E, Shamsazar A. Immunoinformatics-guided Design and Structural Validation of a Multi-epitope Vaccine Candidate Targeting Gastric Cancer–associated Membrane Proteins. Research in Molecular Medicine. 2026; 14(4):175-190. https://doi.org/10.22034/rmm.14.4.1467.1

https://doi.org/10.22034/rmm.14.4.1467.1

Article Type:
Research Paper

Article info:
Received: 17 Jul 2026
Revised: 02 Oct 2026
Accepted: 20 Oct 2026

Keywords:
Cancer vaccine design, Gastric cancer, Immunoinformatics, Multi-epitope vaccine, Structural vaccinology, T-cell epitopes

ABSTRACT

Background: Epitope-based cancer vaccines require rigorous safety filtering and structural validation to overcome translational limitations in heterogeneous malignancies, such as gastric cancer. This study aimed to design and computationally validate a safety-oriented multi-epitope vaccine targeting gastric cancer–associated membrane proteins.

Materials and Methods: Extracellular domains of nine gastric cancer–associated membrane proteins were screened to identify CTL (9-mer) and HTL (15-mer) epitopes. Peptides with exact sequence matches to the human reference proteome were excluded as a preliminary self-similarity filtering step. Epitope prioritization was performed using NetMHCpan and NetMHCIIpan based on binding affinity and percentile rank. Selected candidates were evaluated for antigenicity, allergenicity, toxicity, proteasomal cleavage, and TAP transport efficiency. High-ranking epitopes were assembled using optimized linkers with an N-terminal β-defensin-3 adjuvant. Physicochemical properties, intrinsic disorder, and secondary structure were analyzed. The tertiary structure was predicted, refined, and validated using Ramachandran plot and TM-score metrics. Vaccine–HLA interactions were assessed by molecular docking and molecular dynamics simulations. Immune responses were simulated in silico, and codon optimization with in silico cloning was performed to evaluate expression feasibility.

Results: Screening of extracellular domains from nine gastric cancer–associated membrane proteins generated 161–900 unique CTL and 109–894 unique HTL peptides per antigen. Six epitopes were prioritized based on low percentile ranks (CTL ≤2; HTL ≤3.1) and favorable antigenicity (VaxiJen 0.51–0.99). The final 143-amino-acid construct had a molecular weight of 15.54 kDa, an instability index of 27.02, and a GRAVY score of −0.435, indicating predicted stability and hydrophilicity. Structural refinement yielded 97.2% of residues in favored or allowed Ramachandran regions, including 90.4% in the core region, with an RMSD of 0.48 Å and a TM-score of 0.9886, confirming the preservation of the global topology. ClusPro docking identified the top-ranked clusters for both complexes, with weighted scores of −881.7 (HLA-A*02:01) and −878.3 (HLA-DR1). Molecular dynamics simulations showed rapid equilibration (~10 ns), stable RMSD, consistent radius of gyration, gradual SASA reduction, and persistent hydrogen bonds. Codon optimization achieved a CAI of 1.0 and a GC content of 50.82%, supporting expression feasibility.

Conclusion: This integrative strategy provides a computationally prioritized and structurally validated multi-epitope vaccine candidate. Nevertheless, the applied filtering strategy represents only a preliminary risk-reduction approach, and all findings require experimental validation.

*** Corresponding Author:**
Reza Safaralizadeh, Professor.
Address: *Department of Animal Biology, Faculty of Natural Sciences University of Tabriz, Tabriz, Iran.*
Phone: *+98 (912) 5140527*
E-mail: *safaralizadeh@tabrizu.ac.ir*

Copyright © 2026 The Author(s);
This is an open access article distributed under the terms of the Creative Commons Attribution License (CC-By-NC 4.0: https://creativecommons.org/licenses/by-nc/4.0/legalcode.en), which permits use, distribution, and reproduction in any medium, provided the original work is properly cited and is not used for commercial purposes.

Introduction

Immunoinformatics-based vaccine design has increasingly been applied to both infectious diseases and cancer due to its ability to computationally predict antigenic determinants and evaluate vaccine candidates prior to experimental validation [1]. One illustrative example is the in silico design of a multiepitope vaccine against *Helicobacter pylori*, in which helper T lymphocyte (HTL) and cytotoxic T lymphocyte (CTL) epitopes were selected based on antigenicity, toxicity, and allergenicity, followed by structural modeling, molecular docking, molecular dynamics simulations, and in silico cloning, with experimental validation proposed as a necessary next step [2].

The induction of coordinated $CD4^+$ and $CD8^+$ T-cell responses is critical for cancer immunotherapy. $CD4^+$ T-cell epitope–based heterologous prime–boost strategies enhance tumor-specific helper T cell responses, expand and diversify $CD8^+$ T cells, and significantly inhibit tumor growth in preclinical models [3]. These findings highlight the relevance of multiepitope vaccine approaches capable of engaging both helper and cytotoxic T-cell compartments.

Multiple studies have applied immunoinformatics pipelines to design therapeutic multiepitope cancer vaccines. Constructs targeting HPV16 and HPV18 E6/E7 oncoproteins were predicted to be antigenic, immunogenic, nonallergenic, and nontoxic, with favorable interactions with innate immune receptors and simulated activation of memory immune cells, although experimental validation remained necessary [4, 5]. Similarly, PD-L1–targeting multi-epitope vaccines incorporating CTL, HTL, and B-cell epitopes demonstrated strong antigenicity, stable interactions with TLR4, and the predicted activation of cellular and humoral immunity [6], highlighting the versatility of computational vaccine design across diverse cancer targets.

Clinical evaluations of peptide-based vaccines in digestive system cancers, including gastric, colorectal, pancreatic, and liver cancers, have demonstrated favorable safety and stability; however, limited immune potency and translational efficacy underscore the need for improved vaccine design strategies [7]. Advances in epitope prediction tools, such as NetMHCpan 4.1 and NetMHCIIpan 4.0, have improved MHC class I and II epitope predictions accuracy across diverse HLA alleles [8-12]; nevertheless, sequence-based predictions alone remain insufficient. Structural modeling and molecular dynamics analyses have emerged as essential approaches for assessing dynamic stability and peptide–HLA interactions, thereby further supporting immunogenicity predictions [13, 14].

Despite these advances, in silico epitope-based vaccine design remains limited by incomplete immune response modeling, restricted structural prediction accuracy, and reliance on experimental validation [1]. Membrane-associated proteins offer attractive immunological targets due to surface accessibility and roles in tumor growth, adhesion, and immune modulation; however, systematic epitope mining across multiple gastric cancer–associated membrane antigens, combined with rigorous safety filtering, processing-aware epitope selection, and structural validation, remains largely unexplored. Many prior studies also lack post-modeling refinement, stereochemical assessment, and quantitative structural alignment, thereby limiting confidence in the predicted vaccine conformations.

This study addressed these limitations by implementing an integrated immunoinformatics pipeline that combines epitope prediction, antigen processing evaluation, exclusion of self-reactive sequences, physicochemical characterization, and structural validation to design a translationally relevant multi-epitope vaccine targeting gastric cancer–associated membrane proteins. Collectively, this framework integrates sequence-based, structural, and immunological analyses, enhancing the robustness and translational relevance of in silico cancer vaccine design [1, 7].

Materials and Methods

Antigen selection and peptide generation

Nine gastric cancer–associated membrane proteins (UniProt IDs: P04626, P00533, P08581, Q9Y5Y9, P15941, Q9NZQ7, P16422, P21860, and P08069) were selected as antigenic sources. Full-length sequences along with annotated extracellular or topological domains were retrieved in JSON format from UniProt. Extracellular regions were extracted and concatenated to serve as the input for peptide generation.

Using an automated R pipeline (R version 4.5.1) incorporating Biostrings (v2.78.0) [15], dplyr (v1.1.4) [16], stringr (v1.6.0) [17], httr (v1.4.7) [18], and jsonlite (v2.0.0) [19], CTL 9-mer and HTL 15-mer peptides were generated. All candidate peptides were systematically screened against the complete human reference proteome (UP000005640) to exclude sequences identical to any human proteins, reducing the likelihood of selecting

highly conserved self-like peptides. The resulting unique CTL and HTL peptide sets were exported in FASTA format for downstream epitope prediction and immunogenicity assessment. Tumor-associated expression patterns of the selected source proteins were evaluated by comparing STAD tumor and normal tissue expression profiles to assess tumor association rather than tumor specificity. Differential expression (log2 fold change) between STAD tumors and normal tissues was obtained from the TCGA-STAD transcriptomic dataset.

Epitope prediction, processing, and safety evaluation

Peptides excluding human-identical sequences that were generated in R were subsequently analyzed for their MHC-binding potential. Class I epitope–HLA binding affinities were predicted using NetMHCpan via IEDB [20] to identify high-affinity 9-mer binders for alleles including HLA-A*02:01, HLA-A*03:01, HLA-A*24:02, HLA-A*26:01, and HLA-B51:01. For class II epitopes, NetMHCIIpan-based sliding-window predictions were conducted for alleles, such as HLA-DRB1*01:01, HLA-DRB1*04:01, HLA-DRB1*08:01, and HLA-DRB1*10:01, as well as selected DQ alleles. Predictions were interpreted using percentile rank–normalized binding scores from eluted ligand models, in accordance with IEDB-recommended epitope prioritization criteria [21]. Peptide antigenicity was assessed using the VaxiJen v2.0 server with a default threshold of 0.5 [22]. Further evaluation included proteasomal cleavage prediction using NetChop 3.0 [23], TAP transport efficiency using TAPPred SVM [24], and immunogenicity scoring. Peptides were screened for allergenicity using AllerTOP v2.1 [25] and toxicity using ToxinPred [26], according to the default, tool-intrinsic scoring criteria. Additionally, C-ImmSim [27] outputs were integrated to identify additional potential MHC class I and II binding cores. Only peptides classified as antigenic, non-allergenic, non-toxic, and possessing favorable proteasomal and TAP profiles were prioritized for inclusion in the vaccine design.

Multi-epitope vaccine construction and physicochemical characterization

A multi-epitope recombinant vaccine was assembled by incorporating β-defensin-3 as an N-terminal adjuvant, followed by three CTL epitopes and three HTL epitopes. An EAAAK linker was used to separate the adjuvant from CTL epitopes, AAY linkers were placed between the CTL epitopes to enhance proteasomal processing, and GPGPG linkers were inserted between the HTL epitopes to facilitate MHC class II presentation. The final amino acid sequence (143 residues) was analyzed using ExPASy ProtParam [28] to determine its molecular weight, theoretical pI, amino acid composition, instability index, aliphatic index, extinction coefficient, and GRAVY, as defined by the tool-intrinsic calculation models. PepCalc was used to determine the net charge at physiological pH, predict solubility, and analyze peptide composition. Secondary structure was predicted using the GOR4 algorithm [29]. Intrinsic disorder propensity was calculated using the long-disorder mode of IUPred2A [30], and ANCHOR analysis was used to identify potential binding-prone disordered segments.

Structural modeling, refinement, validation, docking, and molecular dynamics

Tertiary-structure prediction of the complete vaccine construct was conducted using the Robetta server (RoseTTAFold) [31]. Five de novo models were generated, and model selection was based on global confidence scores and per-residue error estimates provided intrinsically by the server. All generated models were refined using GalaxyRefine [32], and the best model was selected based on the MolProbity score, clash score, root mean square deviation (RMSD), GDT-HA, and the percentage of residues in favored Ramachandran regions, using the default, tool-defined quality metrics. Secondary-structure alterations before and after refinement were evaluated using STRIDE [33], whereas overall structural similarity and alignment between the pre- and post-refinement models were assessed using TM-align [34]. The refined full-length vaccine construct was subjected to exploratory protein–protein docking with HLA-A*02:01 (PDB ID: 1I1Y) and HLA-DR1 (PDB ID: 1DLH) using ClusPro, following receptor preprocessing in ChimeraX 1.8 [35, 36]. This analysis was performed only to explore structural interactions and interface compatibility, rather than to model physiological peptide presentation by HLA molecules. Visualization was performed using PyMOL 3.1.1 [37]. Molecular dynamics (MD) simulations for both MHC–vaccine complexes were performed using the WebGRO server [38]. The systems were simulated using the GROMOS96 43a1 force field and the SPC water model in a triclinic simulation box, neutralized with 0.15 M NaCl, energy-minimized using the steepest-descent algorithm for 5000 steps, equilibrated under NVT and NPT conditions at 300 K and 1 bar, and subjected to a 25 ns production run. System stability was assessed using backbone RMSD, RMSF, Rg, SASA, and hydrogen-bond analyses.

Immune simulation, codon optimization, and in silico cloning

In silico immune simulations were performed using C-ImmSim to assess potential immune responses [27]. Linear B-cell epitope propensity was evaluated based on hydrophilicity profiling, and potential additional MHC class I and II peptide cores were extracted from the simulation outputs. The full-length vaccine sequence was codon-optimized for *Escherichia coli* strain K-12 using JCat [39], followed by sequence refinement with the CyberTory nucleic acid "Massager" tool. The optimized open reading frame (ORF) was then cloned in silico into the pET-6×His/TEV expression vector using VectorBuilder, incorporating a T7 promoter, ribosome binding site, His-tag, TEV cleavage site, and appropriate terminators (Figure 1).

Results

Epitope mining and unique peptide generation

Comprehensive screening of the extracellular regions of gastric cancer–associated membrane proteins yielded a diverse repertoire of T-cell epitopes. Peptides with exact matches to the human reference proteome were excluded before downstream analyses, and the remaining unique CTL (9-mer) and HTL (15-mer) peptides were retained. The number of unique CTL epitopes per protein ranged from 161 for SCN10A to 900 for MET, whereas HTL epitopes ranged from 109 to 894 across the same protein set. Members of the receptor tyrosine kinase family, including MET, ERBB2, EGFR, and ERBB3, contributed more than 65% of the identified CTL and HTL peptides, likely reflecting their larger extracellular domains and complex topologies, which tend to generate dense, overlapping peptide libraries. Smaller or structurally constrained membrane proteins contributed fewer epitopes but provided unique sequences, highlighting the complementary nature of the selected antigen panel (Table 1).

Quantitative MHC-binding performance of selected CTL and HTL epitopes

The reported percentile ranks follow established IEDB benchmarks, where lower values indicate stronger predicted MHC binding and a higher likelihood of biologically relevant epitope presentation, as previously associated with effective antigen processing and immunogenicity. From the extensive epitope pools, six epitopes were prioritized based on low percentile ranks, broad HLA coverage, and predicted antigenicity. Among the CTL epitopes, KLFNVTSTL showed the strongest predicted binding profile, achieving a best percentile rank of 0.03 for HLA-A*02:01 and maintaining a percentile rank of ≤1.7 across the evaluated alleles. SLYNRGFSL demonstrated a minimum percentile rank

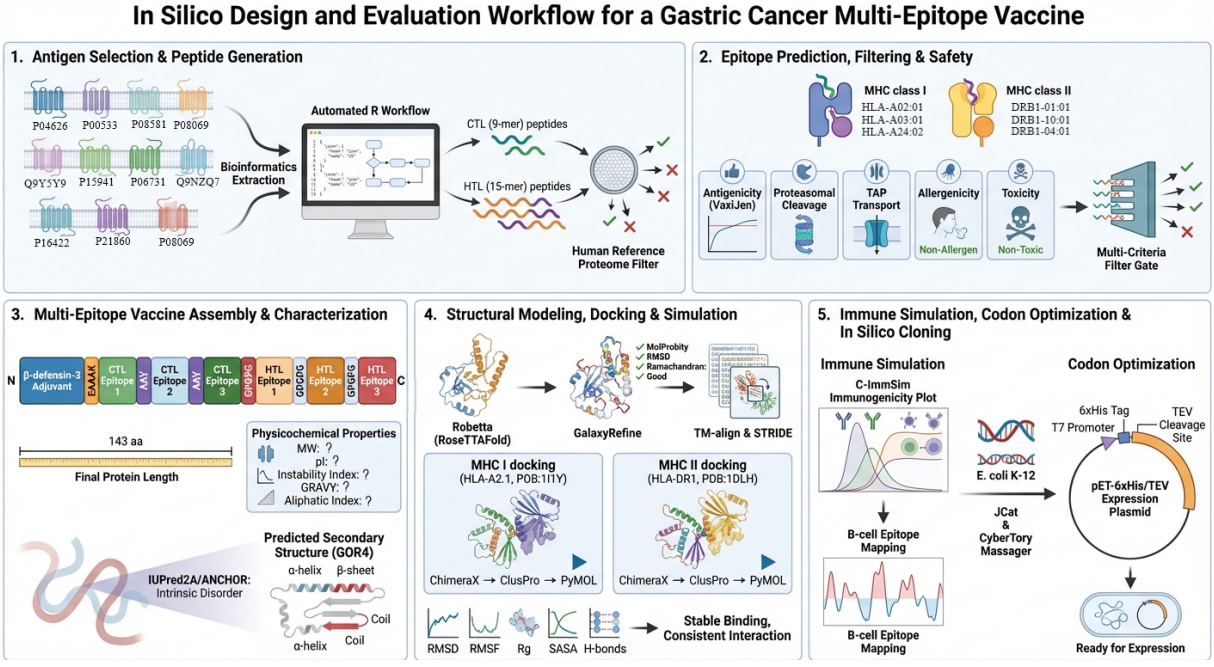


Figure 1. Schematic representation of the in silico multi-epitope vaccine design workflow from antigen selection to immune simulation and in silico cloning

of 0.05 for HLA-A*02:01 and a percentile rank of ≤3.2 across five HLA class I alleles, suggesting moderately consistent affinity. YYLDQKPTV displayed its strongest predicted binding to HLA-A*24:02, with a percentile rank of 0.07, and maintained a percentile rank of ≤1.6 across the associated alleles. These percentile values generally fall within the range associated with a high probability of MHC class I presentation. Antigenicity analysis indicated that KLFNVTSTL had the highest VaxiJen score (0.99), followed by SLYNRGFSL (0.59) and YYLDQKPTV (0.51).

HTL epitopes showed similarly favorable predicted class II binding profiles. DVAYYFEKDVKGESL achieved a minimum percentile rank of 0.02 for HLA-DRB1*04:01 and a percentile rank of ≤3.1 across five HLA-DR and HLA-DQ molecules. EVFNILQAAYVSKPG achieved a minimum percentile rank of 0.05 for HLA-DRB1*01:01 and a percentile rank of ≤2.6 across four alleles, and exhibited the highest antigenicity among the HTL epitopes (0.84). TINWKKLFGTSGQKT showed its strongest predicted binding to HLA-DRB1*01:01, with a percentile rank of 0.82, and retained measurable predicted binding to HLA-DRB1*04:01. Collectively, these results suggest that the selected HTL epitopes may support $CD4^+$ T-cell activation across multiple HLA backgrounds. All selected CTL and HTL epitopes were predicted to be non-toxic by ToxinPred, further supporting the safety profile of the prioritized epitope set (Table 2).

Population coverage analysis further demonstrated that the selected CTL and HTL epitopes provided broader predicted MHC class I coverage than MHC class II coverage across both global and Iranian populations. Worldwide, the estimated MHC class I population coverage ranged from 4.54% to 95.55%, whereas MHC class II coverage ranged from 0% to 56.84%. For the Iranian population, the predicted coverage was 62.88% for MHC class I and 14.68% for MHC class II. These findings suggest that, despite the limited number of selected epitopes, the vaccine candidate is predicted to achieve relatively broad MHC class I population coverage while exhibiting more restricted MHC class II coverage (Figure 2).

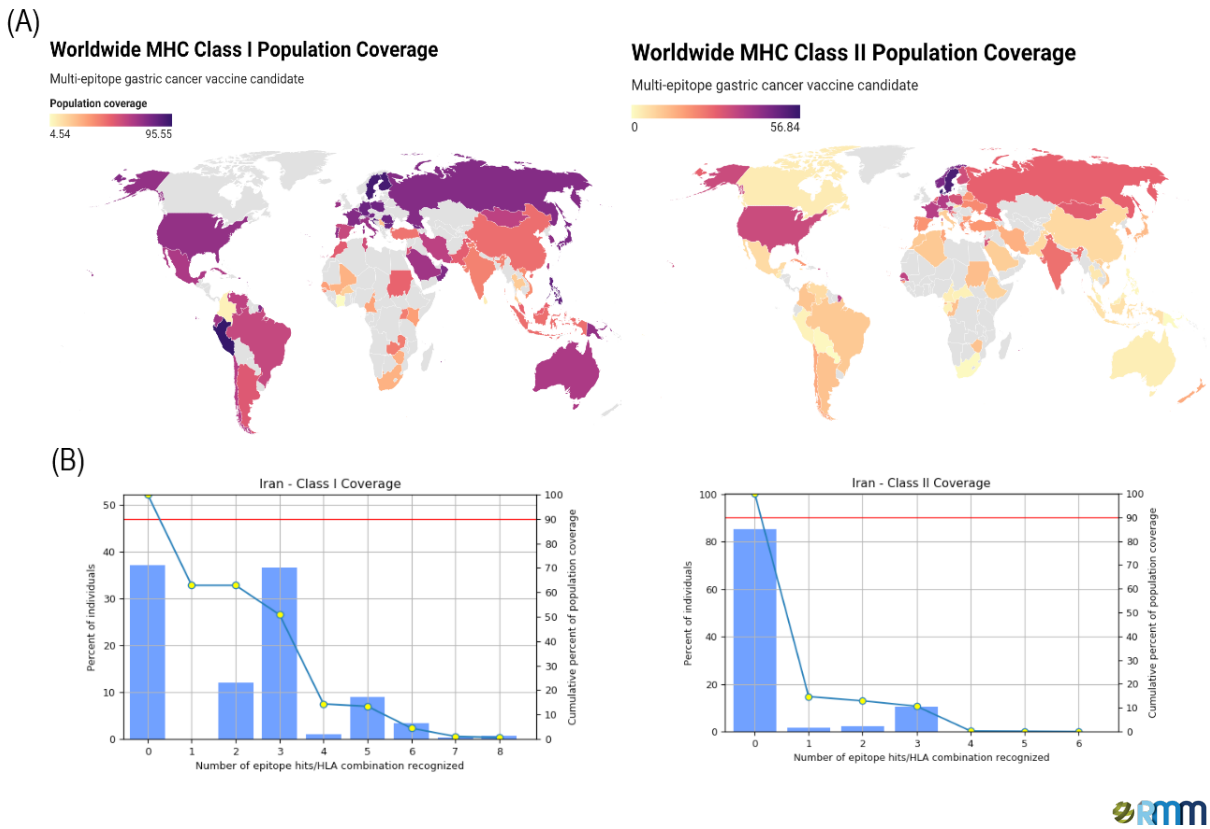


Figure 2. Population coverage analysis of the selected CTL and HTL epitopes

A) Worldwide population coverage maps for MHC class I and MHC class II epitopes, B) Predicted population coverage, average hit, and PC_{90} values for the Iranian population

Note: MHC class I epitopes exhibited substantially broader predicted population coverage than MHC class II epitopes.

Physicochemical properties and secondary-structure composition of the vaccine construct

The complete amino acid sequence of the designed multi-epitope vaccine construct, consisting of 143 residues, is shown below:

GIINTLQKYYCRVRGGRCAVLSCLPKEEQIGKCSTRGRKCCRRKKEAAAKYYLDQKPTVAAYKLFNVTSTLAAYSLYNRGFSLGPGPGDVAYYFEKDVKGESLGPGPGEVFNILQAAYVSKPGGPGPGTINWKKLFGTSGQKT. Within this sequence, residues approximately 23–64 correspond to the β-defensin-3 adjuvant, which was flagged by ToxinPred due to its cationic and antimicrobial nature; however, β-defensin-3 is a well-characterized human-derived immunological adjuvant with established safety profiles in vaccine design studies (Figure 3).

The final vaccine construct had a calculated molecular weight of 15.54 kDa and a theoretical isoelectric point of 9.67, indicating a predominantly basic protein. The instability index was estimated at 27.02, suggesting structural stability under physiological conditions. The GRAVY score of −0.435 reflected an overall hydrophilic nature, consistent with favorable solubility and comparable to values reported for recombinant multi-epitope vaccine constructs with efficient expression and antigen-processing characteristics. Secondary-structure prediction using STRIDE and GOR4 analyses revealed a predominance of random coil conformations (59.4%), followed by α-helices (25.2%) and β-strands (15.4%), indicating a mixed secondary-structure composition with a predominance of coil regions, which is commonly reported for multi-epitope vaccine constructs and may facilitate epitope accessibility. Consistent with these findings, IUPred2A analysis indicated low predicted intrinsic disorder outside the linker regions (Figure 4).

Robetta structure prediction, refinement, and structural alignment validation

Tertiary-structure prediction using Robetta generated five models (residues 1–143), with a moderate overall confidence of 0.51 and per-residue uncertainty mainly in loops and linkers. Refinement with GalaxyWEB produced five optimized models, of which Model 4 was selected because of its superior local quality, as indicated by a GDT-HA of 0.9913, an RMSD of 0.268 Å, a MolProbity score of 1.518, and a clash score of 6.6. Ramachandran analysis of the refined model showed that 97.2% of the residues were located in favored or allowed regions (90.4% in the core, 7.0% in additionally allowed regions, 1.8% in generously allowed regions, and 0.7% in disallowed regions), surpassing the >85% threshold for reliable models (Figures 5A, 5B, and 5C).

Structural consistency between the pre-refined and refined models was assessed using TM-align. Despite moderate confidence in the initial model, the overall fold was largely preserved, with complete alignment across all 143 residues, an RMSD of 0.48 Å, 100% sequence identity, and a TM-score of 0.9886. These findings indi-

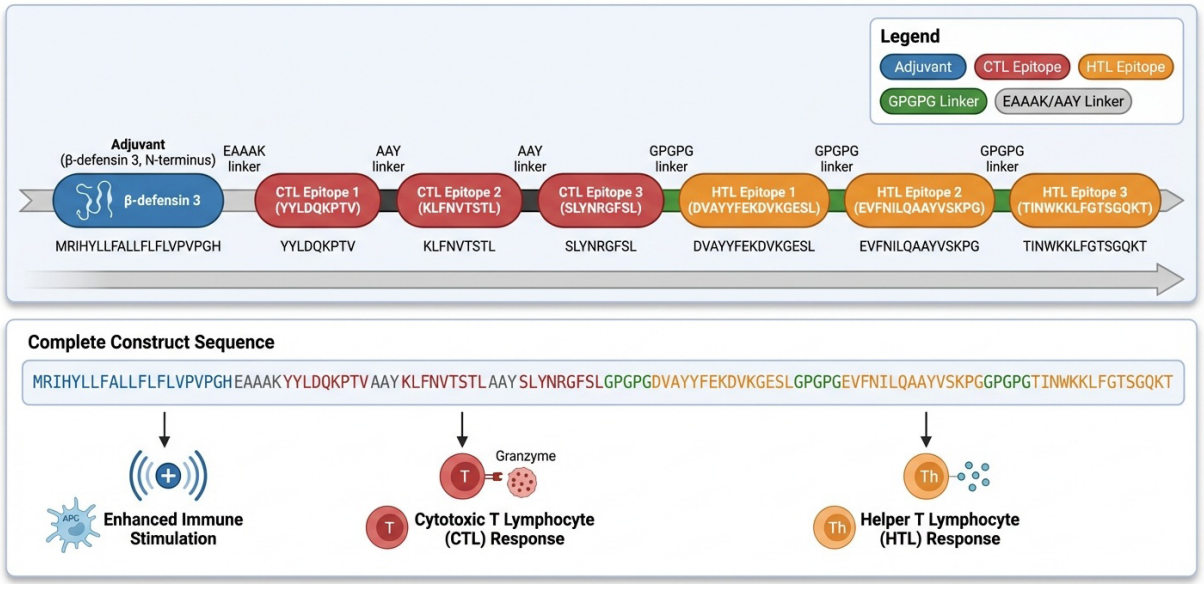


Figure 3. Schematic illustration of the designed multi-epitope vaccine construct showing the adjuvant, CTL and HTL epitopes, linker arrangement, and the expected immune responses

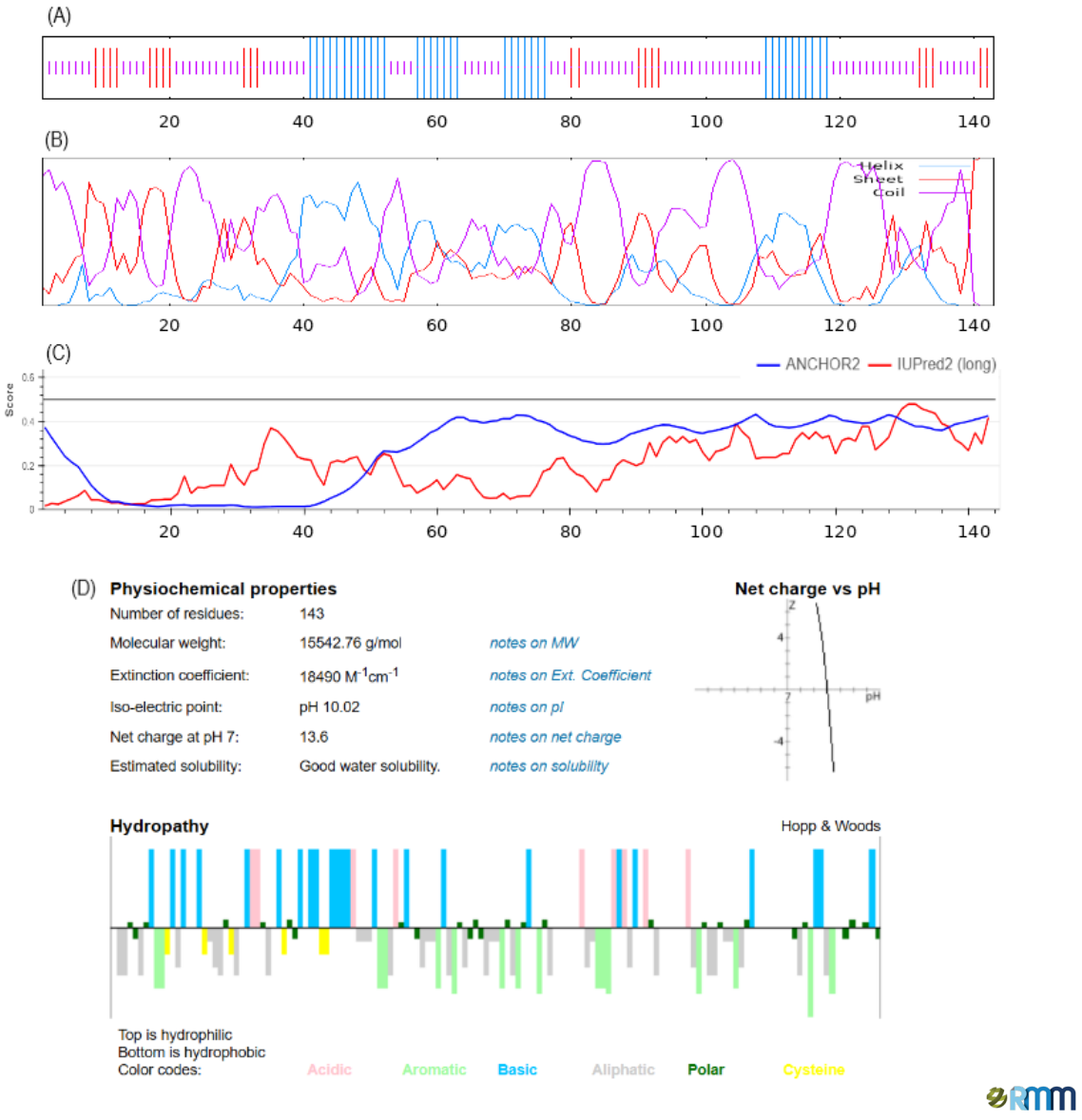


Figure 4. Structural and physicochemical analysis of the designed multi-epitope vaccine

A and B) Secondary-structure prediction of the vaccine construct using GOR4, C) Intrinsic disorder profile predicted by IUPred2A, D) Summary of the predicted physicochemical characteristics of the vaccine construct

cate that refinement primarily improved the local stereochemistry and loop/linker regions without altering the global topology. Collectively, these results confirm the robustness, structural stability, and reliability of the final vaccine model for subsequent docking and molecular dynamics analyses.

Docking energetics and molecular dynamics stability

Protein–protein docking using ClusPro identified Cluster 0 as the most favorable binding mode for both MHC classes. The reported weighted energy scores (−881.7 kcal/mol for the vaccine–HLA-A*02:01 complex with 102 cluster members and −878.3 kcal/mol for the vaccine–HLA-DR1 complex with 85 members) represent relative ClusPro scoring values rather than physical binding free energies and were therefore interpreted comparatively to rank docking poses (Figures 5D and 5E). Molecular dynamics simulations indicated that both complexes reached approximate conformational equilibrium within the first 10 ns of the 25 ns simulation. Backbone RMSD values fluctuated around stable mean levels, while RMSF analysis showed that flexibility was primarily confined to the terminal and loop regions, with comparatively lower fluctuations at the vaccine–MHC interfaces. The radius of gyration values remained stable throughout the simulations, and solvent-accessible sur-

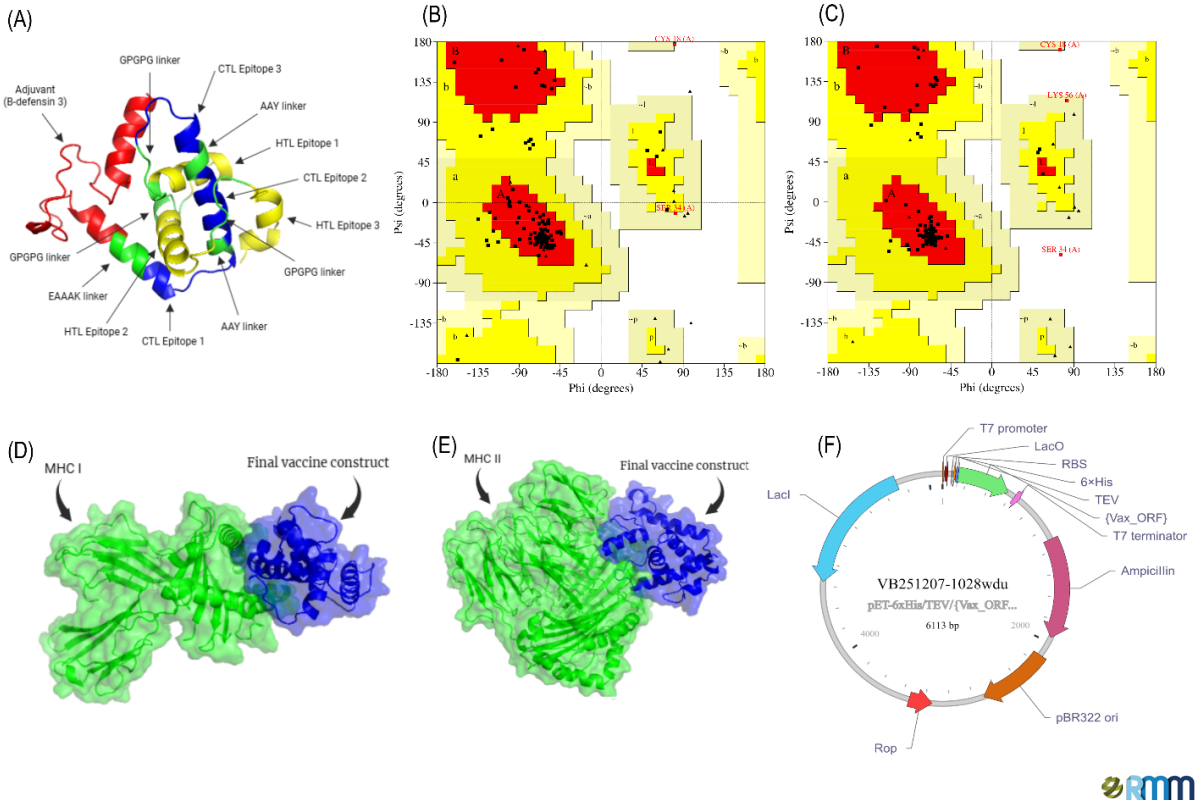


Figure 5. Structural modeling and exploratory docking analysis of the full-length multi-epitope vaccine construct

A) Refined three-dimensional structure, B and C) Ramachandran plots before and after refinement, D) Docking with HLA-A*02:01, E) Docking with HLA-DR1, F) In silico cloning into the pET-6×His/TEV vector

face area exhibited a gradual decrease, consistent with the maintenance of overall structural compactness. Hydrogen-bond counts fluctuated around steady averages, suggesting persistent intermolecular contacts over the simulation period (Figure 6). Because the intact vaccine construct, rather than processed peptide epitopes, was analyzed, these findings indicate structural interactions only and support the dynamic stability of the simulated complexes. However, they should not be interpreted as direct evidence of binding affinity, physiological HLA antigen presentation, or immunogenicity.

Antigen processing, immune simulation, and expression feasibility

NetChop 3.0 predicted 50 proteasomal cleavage sites across the 143–amino-acid vaccine construct, indicating efficient processing potential. All CTL epitopes were flanked by high-confidence terminal cleavage sites (scores up to 0.98), supporting accurate generation of MHC class I–presentable 9-mer peptides, aided by AAY linkers. Cleavage patterns within HTL epitopes and the β-defensin-3 adjuvant suggested effective epitope release, while MHC class II presentation is expected to occur mainly via endosomal pathways. TAP transport predictions identified several epitope-containing nonamer peptides, with high affinity, with some scores exceeding 8.0. Immune simulation indicated four linear B-cell–accessible regions and multiple MHC class II–binding cores clustered centrally, suggesting the potential for coordinated humoral and cellular immune responses (Figure 7). Codon optimization for *E. coli* yielded a codon adaptation index (CAI) of 1.0 and a GC content of 50.82%, and the optimized open reading frame was successfully inserted in silico into the pET-6×His/TEV expression vector, supporting the feasibility of recombinant expression (Figure 5F). Collectively, these quantitative results indicate that the designed multi-epitope vaccine construct may combine high epitope density, favorable MHC binding, structural stability, and expression feasibility, although further experimental validation is warranted.

Discussion

The present study proposes a rigorously filtered, structurally validated multi-epitope vaccine candidate targeting gastric cancer–associated membrane proteins using an integrated immunoinformatics framework. The most salient outcome is the identification and prioritization of

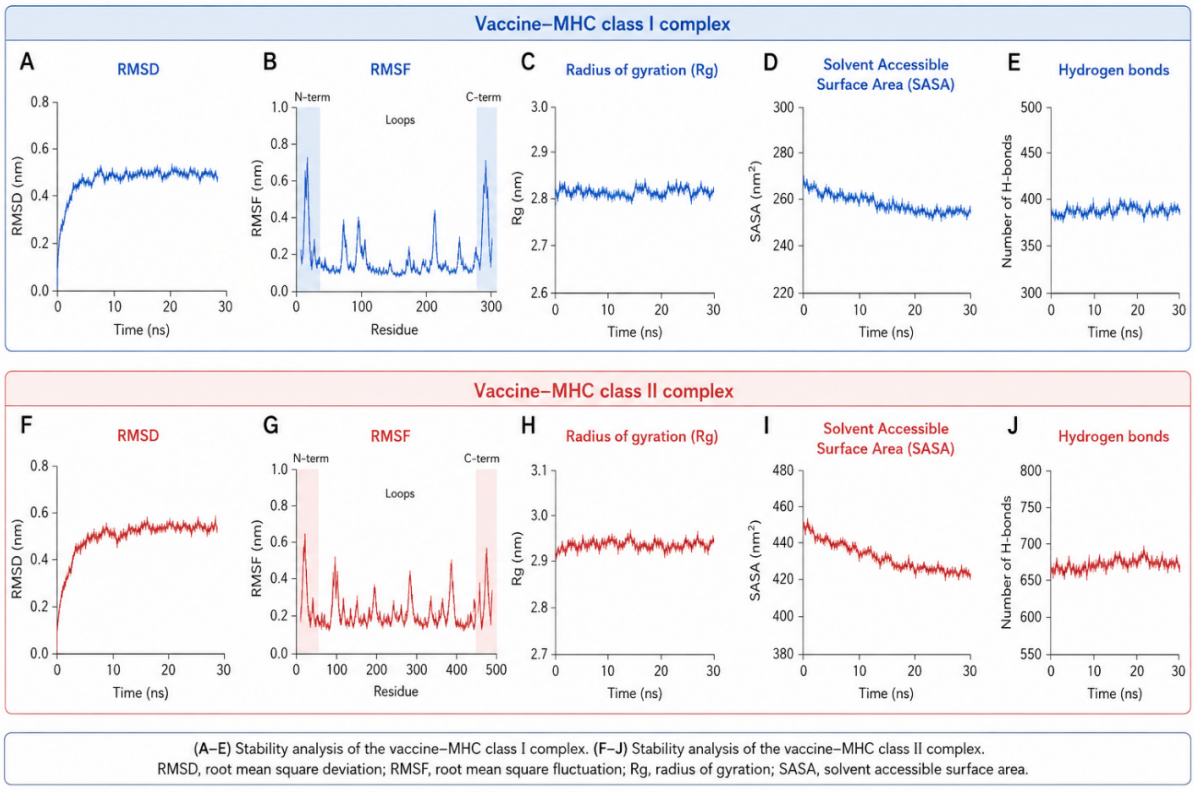


Figure 6. Molecular dynamics analysis of vaccine–MHC complexes during a 25 ns simulation

Note: A–E): The vaccine–MHC class I complex reached rapid equilibration, as indicated by stable backbone RMSD, limited RMSF, stable Rg, slightly decreased SASA, and persistent hydrogen bonds, indicating structural stability. F–J: The vaccine–MHC class II complex showed similar behavior, with stable backbone RMSD, moderate peripheral flexibility, stable Rg, gradually reduced SASA, and sustained hydrogen-bond interactions, supporting overall dynamic stability. These analyses evaluate structural stability only and should not be interpreted as direct evidence of binding affinity, physiological HLA antigen presentation, or immunogenicity.

CTL and HTL epitopes derived exclusively from extracellular regions of clinically relevant tumor-associated antigens, followed by strict elimination of any peptide with exact identity to the human reference proteome. This strategy may reduce the selection of highly conserved self-like sequences; however, exact sequence filtering alone cannot exclude potential cross-reactivity caused by partial similarity or structural mimicry. From an immunoinformatics perspective, the selected epitopes showed favorable predicted MHC class I and II binding profiles across multiple prevalent HLA alleles, as supported by low percentile ranks and high antigenicity scores. Population coverage analysis further indicated that, despite the inclusion of only three CTL and three HTL epitopes, the selected epitope set is predicted to provide broad MHC class I coverage worldwide but comparatively lower MHC class II coverage, with moderate overall population coverage in the Iranian population. These findings support its potential applicability across diverse HLA backgrounds. Epitope selection was based on literature-supported percentile-rank and antigenicity thresholds rather than arbitrary cutoffs, which may contribute to the overall reliability of the design.

Beyond sequence-level predictions, the constructed vaccine exhibited physicochemical properties consistent with stability, solubility, and feasibility for recombinant expression. These properties were supported by its balanced secondary-structure composition and low intrinsic disorder and were consistent with ranges commonly reported in previous immunoinformatics-based cancer vaccine studies. Structural modeling using Robetta, followed by refinement and quantitative validation, yielded a compact and stereochemically reliable conformation with high Ramachandran favorability and near-complete preservation of the global fold after refinement. Docking and 25 ns molecular dynamics simulations supported the structural stability of the full-length vaccine construct in complex with HLA-A*02:01 and HLA-DR1, as indicated by stable backbone RMSD, limited interfacial flex-

Table 1. Biological characteristics, tumor-associated expression, and epitope repertoire of the selected gastric cancer-associated membrane antigens

Protein (UniProt ID)	Localization	GC Evidence	Clinical Relevance	Inclusion Rationale	CTL	HTL	log2FC	TCGA-STAD
ERBB2 (P04626)	PM receptor	Amplified in GC	Trastuzumab target	Accessible surface antigen	622	616	0.69	↑
EGFR (P00533)	PM receptor	Promotes GC progression	Therapeutic target	Extracellular RTK	613	607	0.74	↑
MET (P08581)	PM receptor	Promotes GC invasion	Therapeutic target	Extracellular RTK	900	894	2.13	↑↑
SCN10A (Q9Y5Y9)	PM ion channel	Emerging GC evidence	Exploratory biomarker	Membrane-associated candidate	161	109	0.009	Low
MUC1 (P15941)	PM glycoprotein	Overexpressed in GC	Tumor-associated antigen	Accessible ectodomain	337	337	0.97	↑
CD274 (PD-L1, Q9NZQ7)	PM checkpoint	Immune evasion in GC	ICI biomarker	Immune checkpoint antigen	212	206	0.72	↑
EPCAM (P16422)	PM adhesion	Overexpressed in GC	CSC/diagnostic marker	Highly expressed surface antigen	234	228	2.77	↑↑
ERBB3 (P21860)	PM receptor	HER signaling in GC	Therapeutic target	Extracellular RTK	616	610	1.28	↑
IGF1R (P08069)	PM receptor	Growth signaling in GC	Therapeutic target	Extracellular RTK	187	181	0.46	↑

Abbreviations: PM: Plasma membrane; RTK: Receptor tyrosine kinase; CSC: Cancer stem cell; ICI: Immune checkpoint inhibitor.

Note: ↑: Increased; ↑↑: Strongly increased. Subcellular localization was obtained from UniProt, and tumor-versus-normal expression data were derived from TCGA-STAD. Gastric cancer evidence, clinical relevance, and inclusion rationale were summarized based on the literature reviewed in this study.

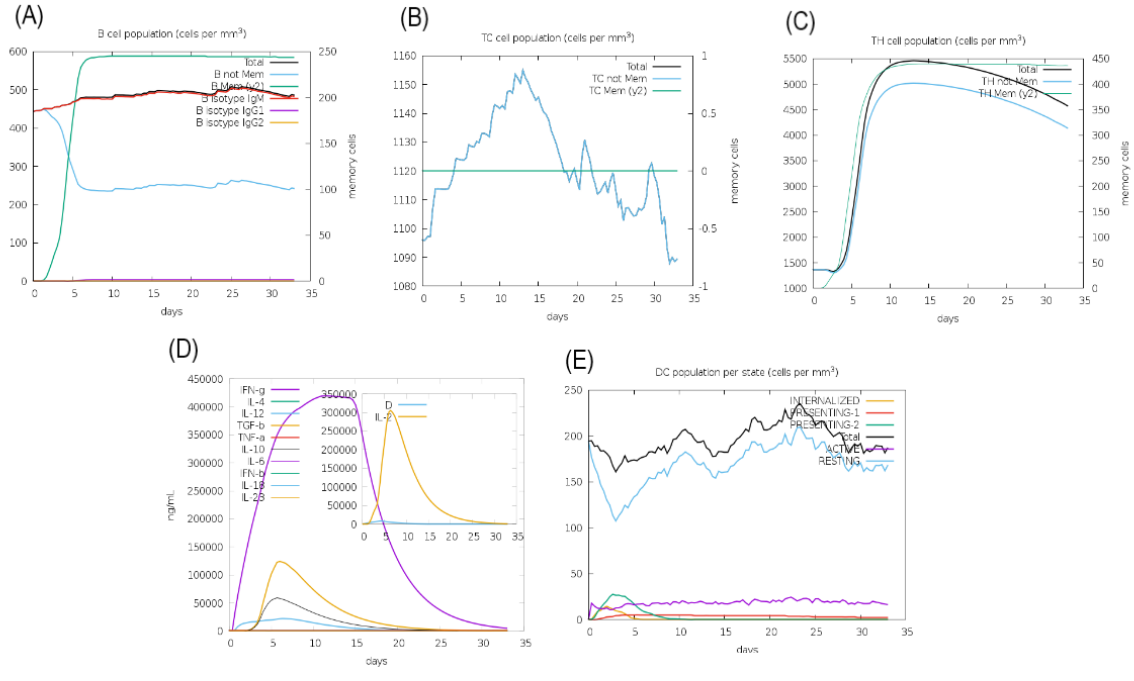


Figure 7. In silico immune simulation of the designed multi-epitope vaccine (C-ImmSim)

A) B cells: Total, memory, and isotype-specific (IgM, IgG1, and IgG2) responses indicate predicted humoral activation, consistent with the predicted linear B-cell epitopes; B) $CD8^+$ T cells: Total and memory counts show moderate cytotoxic activation, reflecting the limited number of incorporated CTL epitopes; C) $CD4^+$ T cells: Total and memory counts exhibit stronger activation, supported by multiple predicted MHC class II epitopes; D) Cytokines: Concentrations and danger-signal profiles indicate the initiation of immune signaling; E) Dendritic cells: Total, active, resting, internalized, and antigen-presenting populations demonstrate effective antigen processing and presentation, collectively suggesting balanced humoral and cellular immunity

Table 2. Characteristics of the prioritized CTL and HTL epitopes selected for the construction of the recombinant multi-epitope vaccine

Epitope	Type	Source Protein	Length (aa)	Predicted HLA Allele(s)	Best Percentile Rank	Antigenicity (VaxiJen)
YYLDQKPTV	CTL	SCN10A	9	HLA-A*02:01, HLA-A*24:02, HLA-A*03:01, HLA-B*51:01	≤1.6	0.51
KLFNVTSTL	CTL	PD-L1 (CD274)	9	HLA-A*02:01, HLA-A*24:02, HLA-A*03:01, HLA-A*26:01	≤1.7	0.99
SLYNRGFSL	CTL	ERBB3	9	HLA-A*02:01, HLA-A*24:02, HLA-A*03:01, HLA-B*51:01, HLA-A*26:01	≤2.0	0.59
DVAYYFEKDVKGESL	HTL	EpCAM	15	HLA-DRB1*01:01, HLA-DRB1*04:01, HLA-DRB1*08:01, HLA-DRB1*10:01, HLA-DQA1*01:01/HLA-DQB1*05:01	≤3.1	0.54
EVFNILQAAYVSKPG	HTL	MET	15	HLA-DRB1*01:01, HLA-DRB1*04:01, HLA-DRB1*10:01, HLA-DQA1*01:01/HLA-DQB1*05:01	≤2.6	0.84
TINWKKLFGTSGQKT	HTL	EGFR	15	HLA-DRB1*01:01, HLA-DRB1*04:01	≤0.82	0.66

ibility, sustained hydrogen bonding, and stable radius of gyration profiles. However, these analyses evaluate structural stability rather than binding affinity. Because HLA molecules naturally present processed peptide epitopes rather than intact proteins, the docking and molecular dynamics results should therefore be regarded only as exploratory structural evidence. Antigen presentation in this study is primarily supported by epitope prediction, HLA-binding, proteasomal cleavage, and TAP transport analyses.

The general immunoinformatics strategy adopted in this work aligns with a growing body of literature demonstrating the utility of multi-epitope vaccine design for cancer and infectious diseases. Ryan et al. employed a similar computational pipeline to design a prophylactic–therapeutic vaccine targeting HPV16/18 oncoproteins and capsid proteins, reporting high antigenicity, favorable structural stability, and strong interactions with immune receptors [40]. While both studies integrate CTL, HTL, and B-cell epitopes, a key distinction lies in antigen origin: Ryan et al. focused on viral antigens with no human homologues, whereas the present study targeted endogenous tumor-associated membrane proteins, necessitating substantially stricter safety filtering.

The importance of rational antigen selection emphasized by Buonaguro is directly reflected in our multi-antigen approach [41]. That review highlighted how antigen prevalence, functional relevance, and immune visibility critically influence vaccine efficacy, while also noting tumor heterogeneity and immune escape as persistent challenges. By incorporating extracellular domains from ten distinct gastric cancer–associated membrane proteins, our design sought to mitigate single-antigen escape mechanisms, although it did not fully resolve interpatient heterogeneity.

Several infectious disease vaccine studies—including those targeting *H. pylori* [42], human coronaviruses [43], NeoCoV [44], Influenza B virus [45], SARS-CoV-2 [46], and monkeypox virus [47]—report comparable outcomes in terms of antigenicity, docking stability, and predicted immune responses. However, these studies typically prioritize epitope-binding affinity and population coverage, often with limited attention to antigen processing constraints or self-homology exclusion. In contrast, the present work integrated proteasomal cleavage and TAP transport predictions, consistent with the foundational work of Larsen et al., who demonstrated that incorporating antigen-processing parameters substantially improves the biological relevance of CTL epitope prediction [48].

The emphasis on helper T-lymphocyte epitopes in this study is particularly notable when considered alongside the findings of Datta et al., who experimentally demonstrated that MHC class II–promiscuous $CD4^+$ T-cell epitopes enhance antitumor immunity and reduce HLA restriction [49]. The comparatively stronger $CD4^+$ T-cell activation predicted by immune simulations in our work aligns with this concept and may be advantageous for sustaining cytotoxic responses, supporting memory formation, and shaping the tumor microenvironment.

Safety considerations further differentiate this study from much of the existing literature. Zanoos et al. showed that short peptide segments derived from con-

served bacterial antigens can share identity with human proteins and potentially trigger autoimmune responses [50]. While their work focused on microbial antigens, the implications are particularly relevant for cancer vaccines targeting self-derived proteins. By excluding all peptides with exact matches in the human proteome prior to epitope prediction, our study adopted a precautionary design principle that goes beyond standard allergenicity and toxicity screening.

From a structural perspective, our workflow is consistent with advances in structural vaccinology and AI-assisted modeling. Reviews by Lim et al. and Zhang et al. emphasize that incorporating three-dimensional structural information improves antigen stability, epitope exposure, and manufacturability [51, 52]. Additionally, the quantitative validation of fold preservation after refinement in our study parallels findings by Alshammari et al., who demonstrated that refined in silico models can retain high structural accuracy when properly validated [53]. Unlike some recent studies that emphasize Toll-like receptor docking and built-in adjuvant comparisons [54-56], our work focused primarily on MHC engagement, reflecting a deliberate prioritization of antigen-presentation fidelity over speculation regarding innate-receptor interactions.

The novelty of this work lies in its multidimensional, safety-oriented vaccine design strategy rather than in any single methodological element. First, the complete exclusion of human-identical peptides at the peptide-generation stage provides a concrete and transparent approach to minimizing the risk of autoreactivity, which is particularly relevant to cancer vaccines targeting self-antigens. Second, the balanced inclusion of both CTL and HTL epitopes, with a deliberate emphasis on MHC class II promiscuity, aligns with emerging evidence highlighting the central role of $CD4^+$ T cells in antitumor immunity [49]. Third, processing-aware epitope prioritization, incorporating proteasomal cleavage and TAP transport predictions, was designed to improve the biological plausibility of epitope selection beyond binding affinity alone [48]. Finally, quantitative structural validation, including TM-align–based fold-preservation analysis, strengthens confidence in the predicted conformation and distinguishes this study from many purely sequence-driven designs.

Several limitations should be acknowledged. The immune simulations and docking analyses remain computational approximations and cannot fully capture tumor-induced immunosuppression, antigen competition, or dynamic HLA expression in patients. The relatively small number of CTL epitopes included may limit cytotoxic breadth, which is reflected in moderate predicted $CD8^+$ T-cell responses. Although exact matches to human sequences were excluded, partial homology and conformational mimicry were not assessed exhaustively. Moreover, innate immune receptor engagement was not explored in depth, and all conclusions remain contingent on experimental validation.

Conclusion

In summary, this study presents a carefully constrained and structurally validated immunoinformatics framework for designing a multi-epitope gastric cancer vaccine. When contextualized within existing computational vaccine literature, the findings are largely concordant with prior reports while addressing specific gaps related to safety filtering, antigen processing, and structural confidence. The results represent a mechanistically informed hypothesis and should not be considered direct evidence of vaccine efficacy or physiological HLA antigen presentation. The presented computational framework may serve as a rational and reproducible basis for future in vitro and in vivo experimental evaluation.

Ethical Considerations

Compliance with ethical guidelines

Ethical approval was not required, as this study involved only computational vaccine design and did not include human or animal subjects.

Funding

This research did not receive any grant from funding agencies in the public, commercial, or non-profit sectors.

Author's contributions

Conceptualization and methodology: Elham Safarzadeh and Ali Shamsazar; Vaccine design, software, formal analysis, and writing the original draft: Kianoush Mohammadi; Supervision, review and editing: Reza Safaralizadeh; Final approval: All authors.

Conflict of interest

The authors declared no conflict of interest.

References

[1] Cernuto F, Maleki A, Russo G, Di Salvatore V, Pappalardo F. In-silico epitope-based vaccines design: progress, challenges and the road ahead. Expert Opin Drug Discov. 2025; 20(12):1701-12. [DOI:10.1080/17460441.2025.2599178] [PMID]

[2] Shojaeian A, Sanami S, Mahmoudvand S, Amini R, Alibakhshi A. Design of a multi-epitope vaccine candidate against Helicobacter pylori in gastric cancer: An immunoinformatic approach. GMS Hyg Infect Control. 2025; 20:Doc27. [DOI:10.3205/dgkh000556] [PMID]

[3] Xiao M, Xie L, Cao G, Lei S, Wang P, Wei Z, et al. CD4+ T-cell epitope-based heterologous prime-boost vaccination potentiates anti-tumor immunity and PD-1/PD-L1 immunotherapy. J Immunother Cancer. 2022; 10(5):e004022. [DOI:10.1136/jitc-2021-004022] [PMID]

[4] Pratiwi SE, Ysrafil Y, Mardhia M, Mahyarudin M, Ilmiawan MI, Trianto HF, et al. A novel therapeutic multiepitope vaccine based on oncoprotein E6 and E7 of HPV16 and HPV18: An in silico approach. BioImpacts. 2024; 14(5):27846. [DOI:10.34172/bi.2024.27846] [PMID]

[5] Bahmani B, Amini-Bayat Z, Ranjbar MM, Masjedi MR, Zarnani AH. An immunoinformatic approach for therapeutic epitope-based peptide vaccine design targeting HPV16-E6. Microbiol Metab Biotechnol. 2021; 4(1):49-64. [DOI:10.22104/armmt.2022.1232]

[6] Mahafujul Alam SS, Mir SA, Samanta A, Nayak B, Ali S, Hoque M. Immunoinformatics based designing of a multi-epitope cancer vaccine targeting programmed cell death ligand 1. Sci Rep. 2025; 15(1):12420. [DOI:10.1038/s41598-025-87063-y] [PMID]

[7] Li J, Wang P. Advances in cancer vaccines for digestive system cancers: A systematic analysis of clinical trials. Cancer Manag Res. 2025; 17:2691-703. [DOI:10.2147/CMAR.S561298] [PMID]

[8] Reynisson B, Alvarez B, Paul S, Peters B, Nielsen M. NetMHCpan-4.1 and NetMHCIIpan-4.0: Improved predictions of MHC antigen presentation by concurrent motif deconvolution and integration of MS MHC eluted ligand data. Nucleic Acids Res. 2020; 48(W1):W449-54. [DOI:10.1093/nar/gkaa379] [PMID]

[9] Sun P, Wang L, Liu Z, Xu Z. Design and immunogenic evaluation of multi-epitope vaccines for colorectal cancer: Insights from molecular dynamics and In-Vitro studies. Front Oncol. 2025; 15:1592072. [DOI:10.3389/fonc.2025.1592072] [PMID]

[10] Haji Allahverdipoor K, Saeedian S, Mardani P, Eslami H. In-silico identification of immunogenic peptide epitopes for the design of a multi-epitope therapeutic vaccine against triple-negative breast cancer. Arch Adv Biosci. 2025; 16(1):1-10. [DOI:10.22037/aab.v16i1.48314]

[11] Pavithran G, Rathi B, Santoshi S. Translational and structural vaccinomics approach to design a multi-epitope vaccine against NOL4 autologous antigen of small cell lung cancer. Immunol Res. 2023; 71(6):909-28. [DOI:10.1007/s12026-023-09404-1] [PMID]

[12] Cao H, Ding F. Development of a CTL epitope-based vaccine targeting tumor antigens in esophageal cancer: An immunoinformatic study. Iran J Biotechnol. 2025; 23(4):e4084. [DOI:10.30498/ijb.2025.509383.4084] [PMID]

[13] Amaya-Ramirez D, Martinez-Enriquez LC, Parra-Lopez C. Usefulness of docking and molecular dynamics in selecting tumor neoantigens. Vaccines (Basel). 2023; 11(7):1174. [DOI:10.3390/vaccines11071174] [PMID]

[14] Debroy B, Chowdhury S, Pal K. Designing a novel multi-antigenic epitope-based vaccine "MarVax" against Marburg virus. J Genet Eng Biotechnol. 2023; 21(1):143. [DOI:10.1186/s43141-023-00575-w] [PMID]

[15] Pagès H, Aboyoun P, Gentleman R, DebRoy S. Biostrings: efficient manipulation of biological strings [R package]. Bioconductor; 2019. [DOI:10.18129/B9.bioc.Biostrings]

[16] Wickham H. dplyr: A grammar of data manipulation [R package]. 2015. [Link]

[17] Wickham H. stringr: Simple, consistent wrappers for common string operations [R package]. Version 1.6.0. 2024. [Link]

[18] Wickham H. httr: Tools for working with URLs and HTTP [R package]. Version 1.4.7. 2023. [Link]

[19] Ooms J. The jsonlite package: A practical and consistent mapping between JSON data and R objects [preprint]. arXiv; 2014. [DOI:10.48550/arXiv.1403.2805]

[20] Vita R, Mahajan S, Overton JA, Dhanda SK, Martini S, Cantrell JR, et al. The immune epitope database (IEDB): 2018 update. Nucleic Acids Res. 2019; 47(D1):D339-D343. [DOI:10.1093/nar/gky1006] [PMID]

[21] Fleri W, Paul S, Dhanda SK, Mahajan S, Xu X, Peters B, et al. The Immune epitope database and analysis resource in epitope discovery and synthetic vaccine design. Front Immunol. 2017; 8:278. [DOI:10.3389/fimmu.2017.00278] [PMID]

[22] Doytchinova IA, Flower DR. VaxiJen: A server for prediction of protective antigens, tumour antigens and subunit vaccines. BMC Bioinformatics. 2007; 8:4. [DOI:10.1186/1471-2105-8-4] [PMID]

[23] Nielsen M, Lundegaard C, Lund O, Keşmir C. The role of the proteasome in generating cytotoxic T-cell epitopes: insights obtained from improved predictions of proteasomal cleavage. Immunogenetics. 2005; 57(1-2):33-41. [DOI:10.1007/s00251-005-0781-7] [PMID]

[24] Peters B, Bulik S, Tampe R, Van Endert PM, Holzhütter HG. Identifying MHC class I epitopes by predicting the TAP transport efficiency of epitope precursors. J Immunol. 2003; 171(4):1741-9. [DOI:10.4049/jimmunol.171.4.1741] [PMID]

[25] Dimitrov I, Bangov I, Flower DR, Doytchinova I. AllerTOP v2: in silico prediction of allergens. J Mol Model. 2014; 20(6):2278. [DOI:10.1007/s00894-014-2278-5] [PMID]

[26] Gupta S, Kapoor P, Chaudhary K, Gautam A, Kumar R; Open Source Drug Discovery Consortium; Raghava GP. In silico approach for predicting toxicity of peptides and proteins. PLoS One. 2013; 8(9):e73957. [DOI:10.1371/journal.pone.0073957] [PMID]

[27] Rapin N, Lund O, Bernaschi M, Castiglione F. Computational immunology meets bioinformatics: The use of prediction tools for molecular binding in the simulation of the immune system. PLoS One. 2010; 5(4):e9862. [DOI:10.1371/journal.pone.0009862] [PMID]

[28] Gasteiger E, Hoogland C, Gattiker A, Duvaud S, Wilkins MR, Appel RD, et al. Protein identification and analysis tools on the ExPASy server. In: Walker JM, editor. The Proteomics Protocols Handbook. Totowa (NJ): Humana Press; 2005. [DOI:10.1385/1-59259-890-0:571]

[29] Garnier J, Gibrat JF, Robson B. GOR method for predicting protein secondary structure from amino acid sequence. Methods Enzymol. 1996; 266:540-53. [DOI:10.1016/S0076-6879(96)66034-0] [PMID]

[30] Mészáros B, Erdős G, Dosztányi Z. IUPred2A: Context-dependent prediction of protein disorder as a function of redox state and protein binding. Nucleic Acids Res. 2018; 46(W1):W329-37. [DOI:10.1093/nar/gky384] [PMID]

[31] Kim DE, Chivian D, Baker D. Protein structure prediction and analysis using the Robetta server. Nucleic Acids Res. 2004; 32(Web Server issue):W526-31. [DOI:10.1093/nar/gkh468] [PMID]

[32] Heo L, Park H, Seok C. GalaxyRefine: Protein structure refinement driven by side-chain repacking. Nucleic Acids Res. 2013; 41(Web Server issue):W384-8. [DOI:10.1093/nar/gkt458] [PMID]

[33] Heinig M, Frishman D. STRIDE: A web server for secondary structure assignment from known atomic coordinates of proteins. Nucleic Acids Res. 2004; 32(Web Server issue):W500-2. [DOI:10.1093/nar/gkh429] [PMID]

[34] Zhang Y, Skolnick J. TM-align: A protein structure alignment algorithm based on the TM-score. Nucleic Acids Res. 2005; 33(7):2302-9. [DOI:10.1093/nar/gki524] [PMID]

[35] Meng EC, Goddard TD, Pettersen EF, Couch GS, Pearson ZJ, Morris JH, et al. UCSF ChimeraX: Tools for structure building and analysis. Protein Sci. 2023; 32(11):e4792. [DOI:10.1002/pro.4792] [PMID]

[36] Jones G, Jindal A, Ghani U, Kotelnikov S, Egbert M, Hashemi N, et al. Elucidation of protein function using computational docking and hotspot analysis by ClusPro and FTMap. Acta Crystallogr D Struct Biol. 2022; 78(Pt 6):690-7. [DOI:10.1107/S2059798322002741] [PMID]

[37] Schrödinger LLC. The PyMOL molecular graphics system, version 1.8. New York: Schrödinger LLC; 2015. [Link]

[38] Abraham MJ, Murtola T, Schulz R, Páll S, Smith JC, Hess B, et al. GROMACS: High performance molecular simulations through multi-level parallelism from laptops to supercomputers. SoftwareX. 2015; 1-2:19-25. [DOI:10.1016/j.softx.2015.06.001]

[39] Grote A, Hiller K, Scheer M, Münch R, Nörtemann B, Hempel DC, et al. JCat: A novel tool to adapt codon usage of a target gene to its potential expression host. Nucleic Acids Res. 2005; 33(Web Server issue):W526-31. [DOI:10.1093/nar/gki376] [PMID]

[40] Ryan N, Pratiwi SE, Mardhia M, Ysrafil Y, Liana DF, Mahyarudin M. Immunoinformatics approach for design novel multi-epitope prophylactic and therapeutic vaccine based on capsid proteins L1 and L2 and oncoproteins E6 and E7 of human papillomavirus 16 and human papillomavirus 18 against cervical cancer. Osong Public Health Res Perspect. 2024; 15(4):307-28. [DOI:10.24171/j.phrp.2024.0013] [PMID]

[41] Buonaguro L, Tagliamonte M. Selecting target antigens for cancer vaccine development. Vaccines (Basel). 2020; 8(4):615. [DOI:10.3390/vaccines8040615] [PMID]

[42] Ru Z, Yu M, Zhu Y, Chen Z, Zhang F, Zhang Z, et al. Immunoinformatics-based design of a multi-epitope vaccine with CTLA-4 extracellular domain to combat Helicobacter pylori. FASEB J. 2022; 36(4):e22252. [DOI:10.1096/fj.202101538RR] [PMID]

[43] Kumar A, Rathi E, Kini SG. Computational design of a broad-spectrum multi-epitope vaccine candidate against seven strains of human coronaviruses. 3 Biotech. 2022; 12(9):240. [DOI:10.1007/s13205-022-03286-0] [PMID]

[44] Aziz S, Waqas M, Halim SA, Ali A, Iqbal A, Iqbal M, et al. Exploring whole proteome to contrive multi-epitope-based vaccine for NeoCoV: An immunoinformtics and in-silico approach. Front Immunol. 2022; 13:956776. [DOI:10.3389/fimmu.2022.956776] [PMID]

[45] Wu H, Zhao C, Cheng Z, Huang W, Yu Y. In silico epitope-based peptide vaccine design against influenza B virus: An immunoinformatics approach. Processes. 2025; 13(3):681. [DOI:10.3390/pr13030681]

[46] Khamjan NA, Lohani M, Khan MF, Khan S, Algaissi A. Immunoinformatics strategy to develop a novel universal multiple epitope-based COVID-19 vaccine. Vaccines (Basel). 2023; 11(6):1090. [DOI:10.3390/vaccines11061090] [PMID]

[47] Sanami S, Nazarian S, Ahmad S, Raeisi E, Tahir Ul Qamar M, Tahmasebian S, et al. In silico design and immunoinformatics analysis of a universal multi-epitope vaccine against monkeypox virus. PLoS One. 2023; 18(5):e0286224. [DOI:10.1371/journal.pone.0286224] [PMID]

[48] Larsen MV, Lundegaard C, Lamberth K, Buus S, Brunak S, Lund O, et al. An integrative approach to CTL epitope prediction: A combined algorithm integrating MHC class I binding, TAP transport efficiency, and proteasomal cleavage predictions. Eur J Immunol. 2005; 35(8):2295-303. [DOI:10.1002/eji.200425811] [PMID]

[49] Datta J, Xu S, Terhune JH, Rosemblit C, Berk E, Fitzpatrick E, et al. Novel strategy to identify MHC class II-promiscuous CD4+ peptides from tumor antigens for utilization in vaccination. J Immunother Cancer. 2014; 2(Suppl 3):P234. [DOI:10.1186/2051-1426-2-S3-P47]

[50] Zanoos KA, Nassrullah OJ, Mubarak SMH, Khalesi B, Rahbar MR, Zare Y, et al. OmpA virulence factor, a promising conserved vaccine candidate against Acinetobacter baumannii, could trigger autoreactive immune responses in susceptible population. BMC Immunol. 2025; 26(1):85. [DOI:10.1186/s12865-025-00766-9] [PMID]

[51] Zhang G, Liu C, Li W, Lu J, Li A, Zhu L. Beyond evolution: De novo designed protein toolkit rewriting the rules of synthetic biology. Biosaf Health. 2025; 7(5):306-11. [DOI:10.1016/j.bsheal.2025.09.004] [PMID]

[52] Lim CP, Leow CH, Lim HT, Kok BH, Chuah C, Oliveira JIN, et al. Insights into structural vaccinology for universal coronavirus vaccine development. Clin Exp Vaccine Res. 2024; 13(3):202-17. [DOI:10.7774/cevr.2024.13.3.202] [PMID]

[53] Alshammari M, He J, Wriggers W. Refinement of alphafold2 models against experimental cryo-EM density maps at 4-6Å resolution. Proceedings (IEEE Int Conf Bioinformatics Biomed). 2022; 2022:3423-30. [DOI:10.1109/BIBM55620.2022.9995676] [PMID]

[54] Lei Y, Zhao F, Shao J, Li Y, Li S, Chang H, et al. Application of built-in adjuvants for epitope-based vaccines. PeerJ. 2019; 6:e6185. [DOI:10.7717/peerj.6185] [PMID]

[55] Sethi G, Varghese RP, Lakra AK, Nayak SS, Krishna R, Hwang JH. Immunoinformatics and structural aided approach to develop multi-epitope based subunit vaccine against Mycobacterium tuberculosis. Sci Rep. 2024; 14(1):15923. [DOI:10.1038/s41598-024-66858-5] [PMID]

[56] Zhou P, Shi X, Xia J, Hu H. In silico design and in vitro validation of a multi-epitope peptide vaccine targeting triple-negative breast cancer. Front Oncol. 2025; 15:1611991. [DOI:10.3389/fonc.2025.1611991] [PMID]

This Page Intentionally Left Blank